



HAL
open science

Review of chemical models and applications in Geant4-DNA: Report from the ESA BioRad III Project

Hoang Ngoc Tran, Jay Archer, Gérard Baldacchino, Jeremy M C Brown,
Flore Chappuis, Giuseppe Antonio Pablo Cirrone, Laurent Desorgher, Naoki
Dominguez, Serena Fattori, Susanna Guatelli, et al.

► To cite this version:

Hoang Ngoc Tran, Jay Archer, Gérard Baldacchino, Jeremy M C Brown, Flore Chappuis, et al..
Review of chemical models and applications in Geant4-DNA: Report from the ESA BioRad III Project.
Medical Physics, 51 (9), pp.5873-5889, 2024, 10.1002/mp.17256 . cea-04616961

HAL Id: cea-04616961

<https://cea.hal.science/cea-04616961v1>

Submitted on 19 Jun 2024

HAL is a multi-disciplinary open access archive for the deposit and dissemination of scientific research documents, whether they are published or not. The documents may come from teaching and research institutions in France or abroad, or from public or private research centers.

L'archive ouverte pluridisciplinaire **HAL**, est destinée au dépôt et à la diffusion de documents scientifiques de niveau recherche, publiés ou non, émanant des établissements d'enseignement et de recherche français ou étrangers, des laboratoires publics ou privés.



Distributed under a Creative Commons Attribution 4.0 International License

Review of chemical models and applications in Geant4-DNA: Report from the ESA BioRad III Project

Hoang Ngoc Tran¹  | Jay Archer²  | Gérard Baldacchino^{3,4} |
 Jeremy M. C. Brown⁵ | Flore Chappuis⁶ | Giuseppe Antonio Pablo Cirrone^{7,8}  |
 Laurent Desorgher⁶ | Naoki Dominguez⁹  | Serena Fattori⁷  |
 Susanna Guatelli² | Vladimir Ivantchenko¹⁰ | José-Ramos Méndez⁹ |
 Petteri Nieminen¹¹ | Yann Perrot¹² | Dousatsu Sakata^{2,13,14} | Giovanni Santin¹¹ |
 Wook-Geun Shin¹⁵  | Carmen Villagrasa¹² | Sara Zein¹ | Sebastien Incerti¹ 

¹Univ. Bordeaux, CNRS, LP2I, UMR 5797, Gradignan, France

²Centre For Medical and Radiation Physics, University of Wollongong, Wollongong, New South Wales, Australia

³Université Paris-Saclay, CEA, LIDYL, Gif-sur-Yvette, France

⁴CY Cergy Paris Université, CEA, LIDYL, Gif-sur-Yvette, France

⁵Optical Sciences Centre, Department of Physics and Astronomy, School of Science, Swinburne University of Technology, Melbourne, Australia

⁶Institute of Radiation Physics (IRA), Lausanne University Hospital and University of Lausanne, Lausanne, Switzerland

⁷Istituto Nazionale di Fisica Nucleare (INFN), Laboratori Nazionali del Sud (LNS), Catania, Italy

⁸Centro Siciliano di Fisica Nucleare e Struttura della Materia, Catania, Italy

⁹Department of Radiation Oncology, University of California San Francisco, San Francisco, California, USA

¹⁰CERN, Geneva, Switzerland

¹¹European Space Agency, ESTEC, Noordwijk, The Netherlands

¹²Institut de Radioprotection et de Sûreté Nucléaire (IRSN), Fontenay-aux-Roses, France

¹³Division of Health Sciences, Osaka University, Osaka, Japan

¹⁴School of Physics, University of Bristol, Bristol, UK

¹⁵Physics Division, Department of Radiation Oncology, Massachusetts General Hospital & Harvard Medical School, Boston, Massachusetts, USA

Correspondence

Hoang Ngoc Tran, Univ. Bordeaux, CNRS, LP2I, UMR 5797, F-33170 Gradignan, France.
 Email: tran@lp2ib.in2p3.fr

Funding information

ESA/BioRad3, Grant/Award Numbers: 4000132935/21/NL/CRS, NIH/NCI R01CA187003, R01CA266419

Abstract

A chemistry module has been implemented in Geant4-DNA since Geant4 version 10.1 to simulate the radiolysis of water after irradiation. It has been used in a number of applications, including the calculation of G-values and early DNA damage, allowing the comparison with experimental data. Since the first version, numerous modifications have been made to the module to improve the computational efficiency and extend the simulation to homogeneous kinetics in bulk solution. With these new developments, new applications have been proposed and released as Geant4 examples, showing how to use chemical processes and models. This work reviews the models implemented and application developments for modeling water radiolysis in Geant4-DNA as reported in the ESA BioRad III Project.

KEYWORDS

Geant4-DNA, radiation chemistry, water radiolysis

1 | INTRODUCTION

Radiation chemistry is the study of the chemical effects of radiation on matter, including the indirect induction of damage to the biological medium through chemical reactions with DNA or other biomolecules. The vast majority of such molecules are immersed in liquid water. They are affected by ionizing radiation through the dissociation of water into chemical species, also known as radiolysis. Understanding how radiolytic species are formed and evolve over time in water is, therefore, essential for studying the biological effects induced by ionizing radiation.

The Monte Carlo technique has proved to be a powerful method for describing the complex kinetics of species diffusion and reactions along ionizing particle tracks. Several Monte Carlo-based software packages have been developed to date as track-structure codes, such as PARTRAC,¹ RITRACKS,² TRAX-CHEM,³ CHEM-KURBUC,^{4,5} IONLYS-IRT,⁶ NOTRE DAME,⁷ TOPAS-nBio,⁸ and Geant4-DNA.^{9–12} The exhaustive lists of these codes are provided by Kyriakou et al.¹³ and Plante.¹⁴ These codes have made it possible to link the fate of physical interactions and the macroscopic observables obtained in radiolysis experiments. Some of these codes also provide biological geometries and tools for simulating direct and indirect DNA damage.

Geant4-DNA,^{9–12} which is fully included in the general-purpose Geant4 Monte Carlo toolkit,^{15–17} simulates early biological damage induced by ionizing radiation at the DNA scale. On-going developments of Geant4-DNA include track structure models in liquid water and other biological materials,^{18–20} physico-chemical and chemical processes for water radiolysis (e.g., refs. 21–23), multi-scale biological geometries and quantification of early DNA damage (such as single-strand breaks, double-strand breaks, base oxidation, etc..., e.g., ref. 13). Water radiolysis induced by ionizing radiation was first introduced in Geant4 10.1 by Karamitros et al.^{21,22} This chemistry extension converts low-energy electrons and energy deposits along the physical track into solvated electrons and dissociated water molecules through physico-chemical processes, such as thermalization, solvation of sub-excitation electrons, electronic hole migration, electron attachment, and dissociation of water molecules, leading to the formation of several reactive species. These radiolytic species are initially distributed heterogeneously in radiation-induced spurs along the tracks of ionizing particles. The spur evolution is described by particle-based Brownian dynamics, in which chemical species are considered as individual particles with specific properties such as charge, velocity, and mass. These chemical species diffuse through the medium and react with each other or with the solvent medium.

The encounter of these chemical species can be simulated either by many diffusion steps up to a reaction using the Step-by-Step (SBS) model or by an independent pair approximation using the Independent Reaction Time (IRT) model, as described in detail below. The effects of scavengers were recently integrated into Geant4-DNA^{23,24} in Geant4 version 11.1. These effects are introduced into the chemical stage of water radiolysis by defining scavenger-specific chemical reactions and the concentration of scavengers.

Particle-based models describe the spatial evolution in liquid water of the spur in the heterogeneous phase up to a few microseconds. However, at longer time scales, species and their products disperse and distribute more homogeneously. Under these conditions, particle-based models are less efficient, especially when simulations involve a large number of species. Stochastic and deterministic models have been proposed to extend water radiolysis applications beyond the microsecond scale.^{22–27} The implementation of these models is currently ongoing in Geant4-DNA.

In this paper, we highlight the main developments of the Geant4-DNA chemistry module over the last 10 years, from Geant4 10.1 (2013) to Geant4 11.2 (2023). Section 2 deals with the general design of the chemistry module and its integration into Geant4. Sections 3 and 4 describe and discuss in detail the approaches and methods of the physico-chemical and chemical processes involved. Section 5 highlights applications of the chemistry models of Geant4-DNA.

2 | GENERAL DESIGN OF THE SOFTWARE

As an extension to Geant4, Geant4-DNA benefits from Geant4's flexible and powerful kernel design to implement physical processes and models for track-structure simulations. This design has also been used in the chemistry module, where chemical species are represented as points or particles with specific properties such as name, mass, and charge, ... These entities diffuse within the water-based solvent, which is considered a continuous medium. In this particle-continuum model, the position of the species of interest is explicitly computed as a function of time until the molecules dissociate, recombine, or react with other molecules. In the computational implementation, the evolution of the system is driven by a main instance created by the *G4Scheduler*, which encompasses two distinct processes known as *G4ITStepProcessor* and *G4ITModelProcessor* (Figure 1). IT stands for Interacting Tracks. These two main processes are described as follows:

- *G4ITStepProcessor* manages the physico-chemical processes (electron-hole recombination and

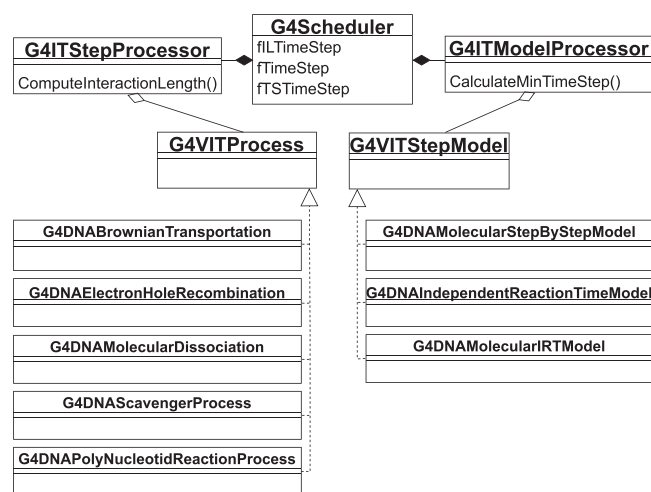


FIGURE 1 Class diagram of the physico-chemistry/chemistry software design in Geant4.

ionized/excited water dissociation) and the Brownian species diffusion process. These processes were implemented via the *G4VITProcess* intermediate interface derived from the general *G4VProcess* interface. Like the physical particle interaction processes in Geant4, individual molecules of all chemical species are tracked through a series of *G4Track* steps. Before each step, *G4Track* provides information on the molecules to *G4VITProcess* to compute the probabilities of all processes. Once a process is selected, its *DoIt* (one of *AtRestDoIt()*, *PostStepDoIt()*, or *AlongStepDoIt()*) method is called and *G4Track* is updated, in the same way as for any Geant4 physical process. The *G4VITProcess* interface provides users with extensive capabilities for implementing new chemical interactions with the medium, including the scavenger reaction process (*G4DNAScavengerProcess*) and the interaction of radical species with DNA geometries (*G4DNAPolyNucleotideReactionProcess*).

- *G4ITModelProcessor* specifically manages collisions (or reactions) between molecules. This singleton class handles chemical reaction models and provides an interface for implementing new reaction models. Like the *G4ITStepProcessor*, it collects all *G4Track* information to compute reaction probabilities. If a reaction condition is met, the reactants are killed and their products are created in the reaction site. The step-by-step model (*G4DNAMolecularStepByStepModel*), the independent reaction time model (*G4DNAMolecularIRTimeModel*), and the synchronized independent reaction time model (*G4DNAIndependentReactionTimeModel*) have been implemented via this interface. These models are further described in Section 4.

At each step of the simulation, the *G4ITStepProcessor* and *G4ITModelProcessor* pro-

cesses are called by *G4Scheduler* to provide information to a stepping algorithm that will select the next event to be processed and synchronize the time and position of all individual molecules during the simulation (see Figure 2). This means that if the next step is decided via the *G4ITModelProcessor*, the remaining molecules will be diffused for the duration of the reaction. Their position and time are updated. A geometry navigator also updates state information to track the molecules in the geometry.

Introduced by Karamitros et al.²² in Geant4 10.1, the chemistry module structure has proved, after more than 10 years, that it successfully meets user requirements in terms of performance and extensibility. Several noteworthy features can be highlighted:

- The chemical processes are compatible with Geant4 physics design, allowing users to run the physical, physico-chemical, and chemical stages of radiolysis simulation in a single application. This compatibility with the physical stage also enables the chemistry module to integrate with Geant4 physics list constructors for various applications and to take advantage of numerous features and functionalities, such as multithreading and geometry navigation.
- The independent interfaces of two separate processors (*G4ITStepProcessor* and *G4ITModelProcessor*) allow users to independently extend particle-continuum models (interactions of chemical species with the medium) or implement new reaction models (track collision) without major modification of the underlying structure. These independent components also enhance maintainability.
- The chemistry module incorporates data structures such as k-d trees²² or octrees to optimize the calculation of separation distances between pairs of reactants during simulation. The objective is to compute the encounter probability of each reactant at each time step. By dividing space into smaller subspaces, these data structures help to efficiently locate the closest reactants of a molecule in the respective sub-volume that contains it. Mostly, this prevents the inclusion of reactants that are too far away, as they generally have lower encounter probabilities. This structure is particularly important for the SBS model, as the search for the nearest neighbor is frequently performed.
- The stepping algorithm provides spatio-temporal information that allows users to extend specific applications such as interaction with a scavenging effect.

However, due to the distinct nature of physics and chemistry processes, such a structure may result in some limitations:

- The stepping algorithm requires synchronization of the time and position of each molecule during the

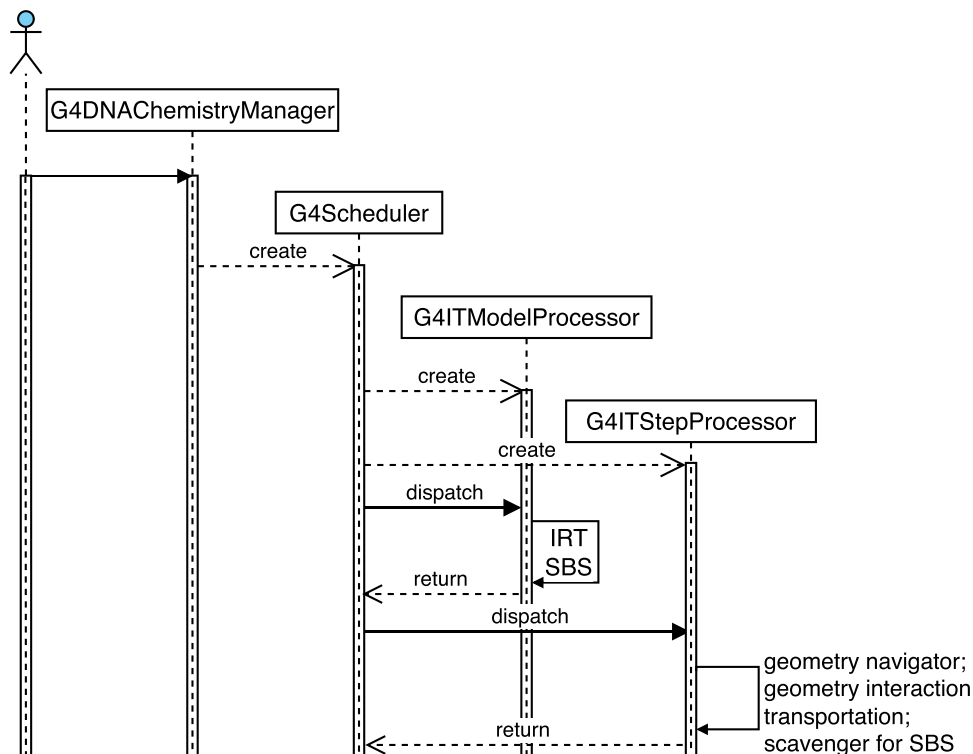


FIGURE 2 Sequence diagram of a Geant4-DNA simulation, modelling the chemical stage. The application instantiates a G4DNAChemistryManager. The local G4Scheduler controls the simulation in each worker thread.

simulation, which can be very time-consuming, especially when dealing with a large number of molecules. The integration of non-synchronized parallel calculations for independent events, commonly used in biochemical models, may pose challenges.

- The Geant4 geometry navigator is designed for the simulation of tracks in particle physics to locate points in the geometry and compute distances to the boundaries of the geometry. This functionality is not well suited to Brownian transportation, which is used for the random steps of chemical molecules. This will lead to unnecessary loss of computation time.

So far, the chemical module of Geant4-DNA provides a useful framework for implementing and extending physical, physico-chemical, and chemical processes/models for various applications of water radiolysis. We will review these processes and models in the next section.

3 | PHYSICO-CHEMICAL STAGE OF WATER RADIOLYSIS

Physico-chemical (also called pre-chemical) processes play a crucial role in determining the distribution of radical species during water radiolysis. The distinction between the physical and physico-chemical stages is

not always clear. Physico-chemical processes become significant when all particles, together with their secondary electrons, have deposited their energy through their track structures during the physical stage, and their energies have decreased to below approximately 8 eV due to excitation and ionization processes. Below this energy, in Geant4-DNA, electrons undergo three sub-excitation processes (Figure 3):

- I. The vibrational excitation process (applicability range from 2 to 100 eV) is based on experimental cross-sections published by Michaud et al.²⁸ for ice targets after a phase-scaling procedure to account for the liquid phase.
- II. The dissociative electron attachment process (4–13 eV) uses experimental results reported by Melton²⁹ (see Section 3.2.3).
- III. The elastic scattering process (four alternative models are available,³⁰ down to a minimum value of 7.4 eV for the Champion model).

The frequency of such electron processes is shown in Figure 3, as a function of electron kinetic energy, obtained with the “option2” Geant4-DNA physics constructor. Note that the vibrational excitation and the dissociative electron attachment processes are not included in “option4” and “option6” Geant4-DNA physics constructors.

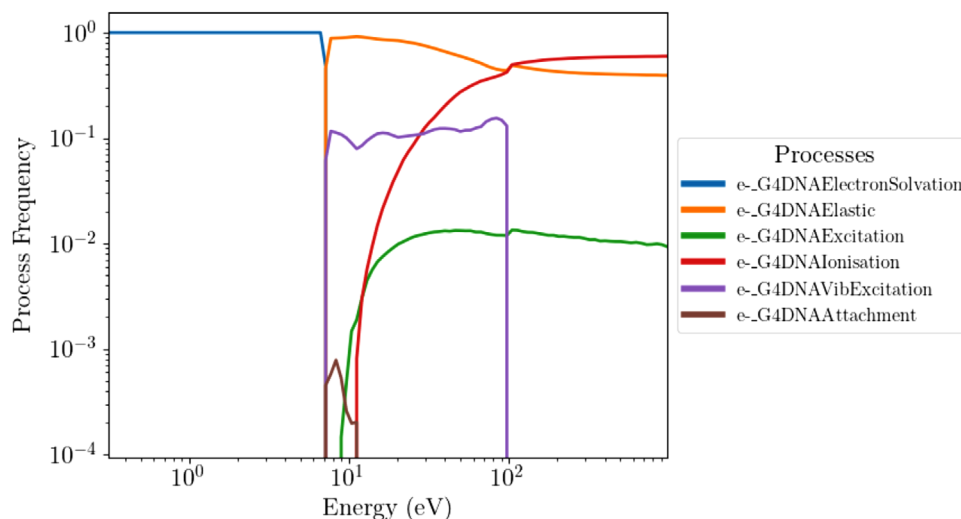


FIGURE 3 Example of normalized process frequency for the Geant4-DNA physics constructor “option2” for incident electrons with energies from 0.3 to 1 keV.

After these energy deposition processes, the physico-chemical stage starts the thermalization process for all secondary electrons and the electronic events in ionized and excited water molecules, which can lead to dissociation.³¹

3.1 | Electron thermalization

The slowed-down sub-excitation electrons will participate in a thermalization process to reach thermal equilibrium (0.025 eV) through multiple interactions with the medium. This process represents a computational burden due to the frequent small energy exchanges of scattering electrons. To reduce the simulation time, Geant4-DNA computes a thermalization distance (*G4DNAElectronSolvation* process) based on experimental data as a function of electron energy, instead of tracking electrons throughout the thermalization process. The electron is then considered to be transported to the point of thermalization, where it is said to be “solvated” or “hydrated” (Figure 3 shows that the only process that is active below 7.4 eV in the Geant4-DNA physics constructor “option2” is the *G4DNAElectronSolvation* process).

Geant4-DNA currently provides five different models for electron thermalization. A detailed review of these models can be found elsewhere in³¹ Briefly,

- The *Meesungnoen2002* model is based on the penetration range simulated by Meesungnoen et al.³² who used the cross-section of Michaud et al.²⁸ for amorphous ice scaled to liquid-phase water. The *Meesungnoen2002* model is used as the default thermalization model in Geant4-DNA.

- The *Terrissol1990* model is based on Michaud and Sanche’s data on sub-excitation cross sections in amorphous-solid water.^{33,34} The paper by Terrissol and Beaudre³⁵ proposes probability density functions of the thermalization distance for electrons in the energy range of 0.2–7 eV.
- The *Ritchie1994* model approximates the relationship between electron energy and the mean value of the “projected range” as a linear correlation with a factor of 1.8 nm/eV, based on experimental data on the projected range of thermalized electrons.³⁶
- The *Meesungnoen2002_amorphous* is an alternative version of Meesungnoen’s penetration range for amorphous ice without the correction for phase influence using cross sections of Michaud et al.²⁸
- The *Kreipl2009* model, proposed by the PARTRAC code,³⁷ uses an exponential probability density function based on the penetration range simulated by Meesungnoen et al.³²

3.2 | Dissociation

Ionized and excited water molecules, induced by primary and secondary particle interactions, participate in a water decomposition process. These highly energized water fragments undergo a breakdown sequence to quickly form primary water radiolysis products, including H_3O^+ , $\cdot\text{OH}$, H^\cdot , OH^- , and H_2 .

3.2.1 | Ionized water molecules

The electron holes in ionized water molecules quickly join the proton transfer processes that occur between

TABLE 1 Dissociation schemes and branching ratios available in the four chemistry constructors (default, option1, option2, option3) of Geant4-DNA.

		Channel	<i>G4EmDNACheckistry_option3</i> constructor ³⁸	<i>G4EmDNACheckistry_default_option1_option2</i> constructors ^{21,22}	Displacement channels (see Table 2)
Branching ratio (%)					
Ionization	H ₂ O ⁺	H ₃ O ⁺ + •OH	100	100	Ionization
		H• + •OH	65	65	A1B1_DissociationDecay
	A ¹ B ₁	H ₂ O + ΔE	35	35	No displacement
		H ₃ O ⁺ + •OH + e _{aq} ⁻	50	55	Auto-ionization
Excitation	B ¹ A ₁	H• + •OH	25.35	–	A1B1_DissociationDecay
		H ₂ + 2•OH	3.25	15	B1A1_DissociationDecay
		2H• + O(³ P) ^a	3.9	–	B1A1_DissociationDecay2
		H ₂ O + ΔE	17.5	30	No displacement
	Rydberg A+B, C+D, Diffuse bands DEA	H ₃ O ⁺ + •OH + e _{aq} ⁻	50	50	Auto-ionization
		H ₂ O + ΔE	50	50	No displacement
		OH ⁻ + •OH + H ₂	100	100	Dissociative attachment
		H• + •OH	35.75	55	A1B1_DissociationDecay
Electron capture	Recombination	H ₂ + 2•OH	13.65	15	B1A1_DissociationDecay
		2H• + O(³ P)	15.6	–	B1A1_DissociationDecay2
		H ₂ O + ΔE	35	30	No displacement

Note: Displacement is indicated as well (see Table 2).

^aOxygen atom in triplet state P.

them and a nearby water molecule, leading to dissociation into H₃O⁺ and •OH molecules. In Geant4-DNA, this dissociation channel is applied at all ionization levels.²¹

3.2.2 | Excited water molecules

Excited water molecules go through several dissociation channels that depend on their excitation levels. Five excitation levels (see Table 1) are simulated in Geant4-DNA. The first and second A¹B₁ and B¹A₁ levels are detailed in different dissociative channels and corresponding branching ratios. The Rydberg series and diffuse band levels are fixed by the branching ratios of 50% for auto-ionization and 50 % for relaxation to the ground state.

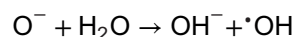
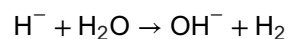
The Geant4-DNA “default”, “option1”, and “option2” chemistry constructors use this dissociation scheme following the PARTRAC code.²¹ To improve accuracy against recent experimental data, Shin et al.³⁸ recently applied the B¹A₁ dissociation channel proposed by the TRACs code, which has been implemented in the “option3” chemistry constructor (*G4EmDNACheckistry_option3*) (see Table 1).

3.2.3 | Electron capture processes

Two different electron capture processes in Geant4-DNA are taken into account for sub-excitation

electrons, leading to the dissociation of the water molecule:

- Dissociative electron attachment (DEA) is the process by which a low-energy electron attaches to a resonant state of the water molecule with a relatively high kinetic energy, leading to a fragment. The kinetic energy at which electron attachment reactions occur is between 4 and 13 eV and can lead to various dissociation processes giving rise to O⁻, H⁻, or OH⁻.²⁹ Modeling these processes is complicated due to the fact that it is extremely difficult to obtain accurate experimental data. The DEA process has been implemented in Geant4-DNA based on Melton’s theoretical calculations on water²⁹ which use a total inelastic cross-section summed over the different dissociation processes. A single dissociation channel is used to produce OH⁻, •OH, and H₂ as the final products of ion-water molecule reactions, according to the following reactions:



- Electron-hole recombination is the process of recombination of the H₂O⁺ ion with a solvated electron, typically occurring within high-concentration regions of radiation-induced spurs. In Geant4-DNA, this process

TABLE 2 Displacement of ionized/excited water and its dissociation fragments, specified as root-mean-square displacement (r_{rms}).

Process	Ionized/excited water molecule r_{rms} (nm)	Products r_{rms} (nm)
Ionization	2.0	0.8
A1B1_DissociationDecay	0	2.4
B1A1_DissociationDecay	0	0.8
B1A1_DissociationDecay2	0	1.6
Auto-ionization	2.0	0.8
Dissociative attachment	0	0.8

is treated as a diffusion process of a nearby thermalized electron (solvated electron) at an appropriate distance from the H_2O^+ ion, leading to dissociation or relaxation to the ground state (see Table 1). The probability of recombination is calculated by an empirical survival fraction³⁹:

$$P(r) = 1 - \exp\left(-\frac{r_c}{r}\right)$$

where r is the distance between the H_2O^+ ion and the solvated electron. The Onsager radius r_c is equal to $e^2/4\pi\epsilon k_B T$, where e is the electron charge, ϵ is the medium permittivity (which is a function of water temperature and density⁴⁰), k_B is Boltzmann's constant and T is the medium temperature. The Onsager radius represents the distance at which the electrostatic energy is equal to the thermal energy of the medium; at temperature $T = 25^\circ C$ and 1 atm, it is about 0.71 nm.

3.2.4 | Displacements of dissociation fragments

Ionized/excited water molecules (called mother molecules) and their dissociation fragments (or daughter molecules) formed from the dissociation scheme also undergo thermalization to release their kinetic energy. As with electron thermalization, this process is simulated by moving the mother and daughter molecules some distance from the initial interaction site. Following the approach described in Kreipl et al.⁴¹ Geant4-DNA calculates the displacement distances (see Table 2) of mother and daughter molecules using empirical root-mean-square (r_{rms}) and momentum conservation:

$$r_{rms} = \sqrt{3}\sigma$$

where σ is the standard deviation of the one-dimensional normal distribution (Gaussian).

In the case of auto-ionization, as introduced by Karamitros et al.^{21,22} Geant4-DNA assumes that the emitted energy of the electrons is 7 eV and, by default,

uses the *Terrisol1990* model (see Section 3.1). An alternative option is available based on the *Kreipl2009* model, which incorporates an energy-dependent mean transport distance of 1 nm using a simplified density function.³⁷ Starting from Geant4 version 10.6, Shin et al.³¹ have implemented an RMS displacement fixed at a thermalization distance of 1.7 eV based on empirical data,⁴² which converts the emitted electron into a solvated one.

Due to the lack of theoretical descriptions and experimental data, one should keep in mind that these models are still not yet fully known or well-validated for liquid water. They are mainly based on experimental data from other materials, scaled to the water phase, or adjusted to match measurable experimental data on chemical radiolysis after 1 ps.⁴¹

In summary, regarding Geant4-DNA physico-chemical models, Geant4-DNA proposes two alternative models (either in the default, option1 and option 2, or in the option3 chemistry constructors, see Table 1). Their impact on radiolysis simulations is described in³¹ and³⁸. For example, as stated in,³⁸ the *G4EmDNACheck_option3* constructor tends to show some better agreement with recent G-value experimental data versus LET. However, more experimental data (e.g., G-values) are still required to fully validate the models.

4 | CHEMICAL STAGE OF WATER RADIOLYSIS

Primary water radiolysis species and solvated electrons are all assumed to be formed within 1 ps. Afterward, it is considered that they are ready to diffuse through Brownian dynamics and eventually react. Due to the initial heterogeneous distributions (spurs) of chemical species at the microscopic scale along the tracks, these evolutions cannot be described using the standard treatment of homogeneous reactions. In Geant4-DNA, microscopic models are used to describe this spur evolution during the chemical stage.

4.1 | Microscopic models

In the microscopic models, we underline the physical assumption that water radiolysis species are particles (or particle-based), whereas water (solvent) is considered as a continuum and the number of reactants involved in the chemical stage must be much smaller than that of the solvent molecules.

4.1.1 | Step-by-Step model

In the Step-by-Step (SBS) model, species are transported in discrete steps (or time steps Δt). The diffusion

process corresponds to Brownian motion, which is described by the solution of the Smoluchowski equation, which can be given in 1D by the following expression²²:

$$p(r, \Delta t | r_0) = \frac{4\pi(r - r_0)^2}{(4\pi D \Delta t)^{3/2}} e^{\left\{ \frac{-(r - r_0)^2}{4D \Delta t} \right\}}, \quad (1)$$

where r_0 is the initial position and r is the next possible position of the species with a probability $p(r, \Delta t | r_0)$ in a time interval Δt . D is the diffusion constant. For each Δt , the displacement of the species is determined by a Gaussian distribution whose endpoint can be calculated by:

$$x(t + \Delta t) = x(t) + R_x \sqrt{2D \Delta t}$$

$$y(t + \Delta t) = y(t) + R_y \sqrt{2D \Delta t}$$

$$z(t + \Delta t) = z(t) + R_z \sqrt{2D \Delta t}$$

where (R_x, R_y, R_z) are random numbers that are normally distributed with zero mean and unit variance. The time step Δt has a lower constraint τ which is defined by the Einstein–Smoluchowski relation:

$$\tau = \frac{mD}{k_B T}$$

where m is the mass of the molecule, k_B is Boltzmann's constant and T is the medium temperature. The time steps over which motion takes place are larger than the time τ , which means that the Smoluchowski equation requires a sufficiently long time for the molecule to relax between collisions with the surrounding medium.⁴³ There is no upper limit to Δt . In geometries with a sufficiently large volume, the only constraint comes from the probability of reactant encounters that may eventually lead to a reaction. If Δt is chosen too large, some reactions may not be modelled and are therefore “missed”. If it is chosen too small, the simulation involves many small time steps, which is very time-consuming. Complexity increases with $O(N_m^2 * N_t)$ where N_m is the total number of molecules and N_t is the number of time steps.²²

Somehow, time steps should depend on the distance between reactant pairs. In Geant4-DNA, Karamitros et al.²² implemented an approach called “dynamic time step” which was initially proposed by Clifford et al.⁴⁴ and Michalik et al.⁴⁵ Briefly, this method proposes a time step model that allows time steps to be chosen as a function of the distance between reactants. Depending on this distance, a probability of reactions that cannot occur with at least 95% (default) confidence is converted into a diffusion time. During this time, the species is considered free to diffuse and may be able to take a long diffusion step. The function in Equation (1) is used to evaluate this diffusion step. This process is repeated

many times until a chemical encounter defines a reaction. Thus, there may be one or more time steps before the reaction occurs. To avoid the scenario of numerous small time steps, the Minimum Time Step technique and the Brownian Bridge technique have been added to limit the number of time steps. While the Minimum Time Step limits the minimum time step allowed for each pair of reactants, the Brownian Bridge technique computes the probability of encounter during their Minimum Time Step and thus compensates for “missed” reactions. The Minimum Time Step values can be increased as a function of the time used in the simulation, using the predefined static time steps proposed by Kreipl et al.⁴¹

The SBS model has been used in the Geant4-DNA “chem1”, “chem2”, “chem3”, and “chem4” user examples, which show how to activate and visualize the chemical track evolution in time and space (refer to Section 5).

4.1.2 | Independent reaction time model

Initially introduced by Clifford et al.⁴⁴ the Independent Reaction Time (IRT) model offers a much more efficient approach than the SBS model. Instead of computing a diffusion time based on the non-reaction probability as in SBS, IRT tends to directly calculate a reaction probability. To achieve this, this model assumes that reactions are independent and that the diffusion of reactants from their initial positions to the reaction site is not influenced by other chemical species or volume boundaries. In this context, based on reaction probabilities and initial spatial positions, reaction times can be sampled for all possible pairs of reactants, sorted by increasing time into a list of possible reactions, and these reactions are processed independently one by one, starting with the reactions with the shortest reaction time without synchronizing time and position of involved species. Products created by reactions in progress can undergo reactions with other reactants and be included in the reaction list.⁴⁴ To account for a reaction, a reaction radius is determined. If the encounter of a pair of reactants at this distance immediately leads to its reaction, this is called a diffusion-controlled reaction (or totally diffusion-controlled reaction). Otherwise, the reaction is determined by a different probability distribution, defined as “a velocity of reaction”. This distribution depends on the encounter distance and reaction rate of the reactant pairs and can be referred to as the Smoluchowski steady-state rate constant. As it does not fully depend on diffusion, this type of reaction is called partially diffusion-controlled. Details of reaction probabilities and their implementation can be found in.^{23,43,46–48}

The IRT model has a much higher computational efficiency than the SBS model, especially when dealing with a large number of species. However, by skipping the computation of diffusion, the spatio-temporal information of the species is not explicitly simulated during

simulation time. Only initial positions and reaction sites are computed.

4.1.3 | Synchronous IRT model

The synchronous IRT (IRT-syn) model proposes an implementation of the IRT model to allow access to spatial-temporal information at certain times. A preliminary prototype version was proposed by Lampe et al.⁴⁹ and a full implementation was released in Geant4 10.7 in 2020.⁴⁸ This implementation uses as the time step the randomly sampled time given by the IRT model until the next expected reaction. In other words, instead of optimizing the time step to the next reaction like the SBS model does, the IRT-syn model calculates the reaction time directly using the IRT model. As a result, each step of the simulation consists of two stages:

- a) The reaction times of all possible pairs of reactants are computed and sorted by time. The lowest reaction times and the corresponding reactions are processed first.
- b) The reactive products are created in the reaction that has taken place and the remaining species are diffused during the time step. Then, depending on their new position, new reaction times are resampled for the next reaction.

This procedure is repeated until the end of the simulation. This means that after each time step, it is necessary to synchronize the time and position of all diffusing species. This is the drawback of IRT-syn. However, thanks to synchronization at each time step, IRT-syn provides users with spatio-temporal information on all species, which can then be coupled with information on geometric boundaries or on the biological target.

4.1.4 | Suitability of microscopic models

In the above review of the microscopic approaches, it is currently not possible to recommend one approach among the others. Indeed, depending on the user application, one model might be more suitable among the SBS, IRT, and IRT-syn. For example, the applicability of SBS and IRT may be different because IRT does not provide spatial information, resulting in much improved speed. SBS will be more adapted if geometries are present in the simulation (SBS gives information on the geometrical location of molecules); IRT instead will be more useful if optimized performance is an issue (for example, in case of high LET simulations, or simulations involving large volumes); finally, IRT-syn is a compromise between the two other approaches. We may only recommend that users try the different models available

in Geant4-DNA (refer to Section 5 for a description of several use cases).

4.2 | Mesoscopic model

The SBS, IRT, and IRT-syn models are well suited to applications involving a small number of chemical species. Computation time remains the main drawback when simulations involve a large number of species or long-time scales. An alternative approach has recently been implemented in Geant4-DNA using the compartment-based representation from Geant4 11.2, which describes the evolution of species by gathering molecules of the same species into a single group placed in a confined volume (or “compartment”).²⁷ Within compartments, the distribution of species is assumed to be homogeneous or “well-mixed”. Individual physical molecules are not simulated. Under these conditions, the compartment-based model proposes that the simulation volume be divided into smaller regions (“voxels”) where species can react with each other within the same voxels, and diffusion is modeled by jumps between adjacent voxels as a first-order reaction. The next sub-volume method (NSM) algorithm⁵⁰ is used to reproduce the possible states of the system, which is described by the Reaction-Diffusion Master Equation (RDME).^{51,52} Since the size of the spurs (produced by distributions of energy deposition by ionizing particles) is comparable to their reaction radius within a few ns after exposure, this period cannot be described using the “well-mixed” model.²¹ Over time, species and their products disperse and distribute more homogeneously when the compartment-based model can be applied to the mesoscopic scale. To distinguish it from microscopic models (or particle-based models), it is called the mesoscopic model (or compartment-based model).

Tran et al.²⁷ have implemented in Geant4-DNA the combination of the SBS model with the mesoscopic model (so-called “SBS-RDME model”). This combination makes it possible to simulate a large number of species and to extend water radiolysis simulations to several seconds after irradiation. In this model, the chemical stage is divided into three sub-stages: the microscopic, mesoscopic, and homogeneous sub-stages. The microscopic sub-stage begins with the formation of species before the start of the chemical stage. When the simulation reaches a time t_1 (about 5 ns), the particle-based SBS simulation is stopped and a uniform Cartesian mesh is initialized for the compartment-based model. This is the start of the mesoscopic sub-stage. The initial resolution of the mesh must be small and chosen according to the spatial distribution of species at the end of the microscopic sub-stage. The hierarchical algorithm of the RDME approach (hRDME) is used to adapt the voxel size to the evolution of the system.⁵³ Over time, mesh voxels will be grouped

into larger voxels resulting in a coarser mesh and containing more homogeneously distributed species. These voxels will eventually merge into one single voxel that covers the entire simulation volume at time t_n , when the homogeneous sub-stage starts. During the homogeneous sub-stage, the chemical master equation (CME) is used to sample only reactive events. Details of this approach can be found in.²⁷

4.3 | Other chemistry features available in Geant4-DNA

4.3.1 | Scavengers

The experimental study of radiation chemistry involves the addition of homogeneously distributed molecules that lead to competing chemical reactions. This allows for control of the production of radio-induced species. These molecules are known as scavengers (see²⁴). Implementing the scavenging effect in the Monte Carlo model poses several problems. The first problem is that, due to the large number of scavenger particles in the system, the scavenging capacity must be a continuum. This was proposed by Pimblott et al.⁵⁴ and Green et al.⁴⁷ to limit the computational cost of the simulations. This continuum approximation assumes that the scavenging particles are homogeneously distributed in the water. However, this leads to an indetermination of the spatial evolution of scavenging molecules in diffusion and reaction with spur species. The high concentration regions of radiation-induced spurs, which introduce the competitive kinetics of radical scavenging and recombination processes, also add to the complexity of the scavenging effect.

In Geant4-DNA, the probability of a radiolytic species interacting with scavengers in the irradiated medium is determined by the following rate equation^{47,54}:

$$\frac{dX}{dt} = -kC_sX$$

where C_s is the scavenger concentration, X is the survival probability of the species and k is the reaction rate. This model is used either for the IRT,²³ the SBS particle-based model,²⁴ or the mesoscopic model. Geant4-DNA provides the “scavenger” example to show how to activate the scavenging process in chemistry using the IRT model. It allows users to define chemical reactions and the concentrations of scavengers by means of a convenient user interface.²⁴

4.3.2 | pH

While the yield of primary radicals from water radiolysis may be expected to be unaffected by pH from 3 to 12^{55,56,57} during heterogeneous distributions of chemical species along tracks, pH affects secondary products

TABLE 3 Acid-base reactions associated with pKa.⁵⁸

#	Equilibrium	pKa
1	$2\text{H}_2\text{O} \leftrightarrow \text{OH}^- + \text{H}_3\text{O}^+$	13.99
2	$\text{H}_2\text{O}_2 + \text{H}_2\text{O} \leftrightarrow \text{HO}_2^- + \text{H}_3\text{O}^+$	11.65
3	$\cdot\text{OH} + \text{H}_2\text{O} \leftrightarrow \text{O}_2^{\cdot-} + \text{H}_3\text{O}^+$	11.90
4	$\text{HO}_2^{\cdot} + \text{H}_2\text{O} \leftrightarrow \text{O}_2^{\cdot-} + \text{H}_3\text{O}^+$	4.57
5	$\text{H}^+ + \text{H}_2\text{O} \leftrightarrow \text{e}^-_{\text{aq}} + \text{H}_3\text{O}^+$	9.77

such as $\text{HO}_2^{\cdot}/\text{O}_2^{\cdot-}$ through various equilibrium processes and the subsequent production of H_2O_2 under atmospheric oxygen conditions.

Indeed, long after irradiation (hundreds of microseconds), the formation and evolution of important biologically relevant species such as $\text{O}_2^{\cdot-}$, HO_2^{\cdot} , and H_2O_2 depend on water pH through a complex equilibrium process involving acid-base reactions. These acid and base concentrations are important to define the HO_2^{\cdot} , $\text{O}_2^{\cdot-}$ and H_2O_2 evolution.

Until Geant4 11.2, Geant4-DNA considers that acid-base equilibrium is constant throughout the simulations. Acid and base concentrations are used to balance the concentrations of chemical species such as $\text{O}_2^{\cdot-}/\text{HO}_2^{\cdot}$ that are created from primary radicals and dissolved oxygen. Table 3 shows the acid-base reactions associated with pKa used to simulate the H_3O^+ and OH^- ions concentrations using the “UHDR” example of Geant4-DNA (see Section 5). pKa is defined as $\text{pKa} = -\log_{10}(\text{Ka})$ where Ka is the value of acid dissociation constant.

However, although a significant change in pH is generally not observed after water irradiation, the alteration of acid-base equilibrium in the microseconds to milliseconds time frame remains an unresolved issue, especially under high dose rate conditions.⁵⁹

4.3.3 | Temperature

In Geant4-DNA, the temperature dependence of water radiolysis, introduced by Karamitros et al.²² is controlled by scaling the rate constants and diffusion coefficients in the reaction-diffusion system. While the modification of rate constants was fitted to the experimental results, the diffusion coefficients were calculated by the Smoluchowski equation with the Debye factor. Details can be found in.^{60,61} Recently, in a user study of temperature-dependent effects using Geant4-DNA, the parameter values were taken from the literature to simulate the evolution of the G-value at different temperatures, ranging from 25°C to 150°C, for incoming MeV electrons.⁵⁵

4.4 | User-friendly interface for input reaction list

Until Geant4 version 11.2, Geant4-DNA provided four chemistry constructors (*G4EmDNACheckistry*, *_option1*,

```

/chem6/TimeStepModel IRT

# species definition
# username [ molecule | charge | D(m2/s) | Radius(nm) ]
#/chem/species O2 [ O2 | 0 | 2.4e-9 | 0.17 ]

/chem/PrintSpeciesTable

# reset reaction table
/chem/reaction/UI

# totally diffusion-controlled (TDC)
/chem/reaction/add H + H -> H2 | Fix | reactionRate[dm3/(mol*s)] | TDC (0)
/chem/reaction/add e_aq + H -> H2 + OHm | Fix | 0.503e10 | 0
/chem/reaction/add e_aq + e_aq -> H2 + OHm + OHm | Fix | 2.50e10 | 0
/chem/reaction/add e_aq + e_aq -> H2 + OHm + OHm | Fix | 0.636e10 | 0
/chem/reaction/add H3Op + OHm -> H2O | Fix | 1.13e11 | 0

# partially diffusion-controlled (PDC)
/chem/reaction/add OH + H -> H2O | Fix | reactionRate[dm3/(mol*s)] | PDC (1)
/chem/reaction/add OH + OH -> H2O2 | Fix | 1.55e10 | 1
/chem/reaction/add e_aq + OH -> OHm | Fix | 0.55e10 | 1
/chem/reaction/add e_aq + OH -> OHm | Fix | 2.95e10 | 1
/chem/reaction/add e_aq + H2O2 -> OHm + OH | Fix | 1.10e10 | 1
/chem/reaction/add e_aq + H3Op -> H + H2O | Fix | 2.11e10 | 1

```

FIGURE 4 User interface for defining chemical species and reactions in the “chem6” example. The time step models are defined exclusively for Step-by-Step (SBS), independent reaction time (IRT), or synchronized IRT (IRT_syn).

_option2, and *_option3*) that offered various lists of reactions involved in water radiolysis and DNA reactions, along with reaction constant data.^{21,23,43,62} Depending on their applications, users can easily introduce new molecules and chemical reactions into chemistry applications to fulfill their simulation needs. The “scavenger”²⁴ and “chem6” examples provide user interfaces to facilitate the addition or removal of chemical reactions. Figure 4 shows a screenshot of the user interface (UI) using the “chem6” example. This UI allows users to include all reactions involved by chemistry constructors or insert their reaction scheme by resetting the reaction table using the command (*/chem/reaction/UI*).

5 | APPLICATIONS

The list of Geant4-DNA chemistry usage examples available in the Geant4 version 11.2 is as follows:

- Using Step-By-Step (SBS) method:
 - The “chem1” extended/medical/dna example illustrates how to activate the simulation of water radiolysis.
 - The “chem2” extended/medical/dna example illustrates how to set the minimum time step limits on water radiolysis.
 - The “chem3” extended/medical/dna example illustrates how to implement user actions in the chemistry module.
 - The “chem4” extended/medical/dna example illustrates how to compute radiochemical yields (“G”)

versus time, including a dedicated ROOT⁶³ graphical interface.

- The “chem5” extended/medical/dna example illustrates how to compute radiochemical yields (“G”) versus time, using alternative physics and chemistry lists.
- The “chem6” extended/medical/dna example illustrates how to compute radiochemical yields (“G”) versus time or LET using the SBS, IRT and IRT_syn methods. User interface is provided for defining chemical species and reactions.
- The “scavenger” extended/medical/dna example illustrates how to simulate scavenging using an easy-to-use interface and the IRT method.
- The “UHDR” extended/medical/dna example illustrates how to activate the chemistry mesoscopic model in combination with the step-by-step model, and allows to simulate chemical reactions beyond 1 μ s post-irradiation.

5.1 | G-value

For comparison with experimental data, one of the most important applications of the Geant4-DNA chemistry module is the calculation of the G-values of water radiolysis. According to the International Commission on Radiation Units,⁶⁴ the yield, $G(x)$ of a chemical species x , is defined by:

$$G(x) = \frac{n(x)}{\varepsilon} .$$

where $n(x)$ is the mean number of chemical species x , created or lost, and $\bar{\epsilon}$ is the mean energy imparted to the matter of that system. Its unit is mol J^{-1} , although the alternative unit molecules per 100 eV of energy deposited is often found in the literature.

The G-values, as calculated in Geant4-DNA, differ somewhat from the ICRU definition. This discrepancy arises because of the time-consuming nature of radiolysis simulations. These simulations are constrained by the microscopic scale, where a short variation of the track is taken into account, and the G-values are therefore calculated for a short-range energy of the ionizing particle. In other words, G-values are determined over a limited range of energies imparted by a single particle. This limitation helps reduce the number of chemical species in the simulation, and subsequently the simulation time. To distinguish the Geant4-DNA definition from the ICRU one, the former will be referred to as the “track segment G-value” or differential yields.⁶⁵

There are two main methods of defining this amount of imparted energy:

- I. The first method is to select a range of energy losses [eLossMin, eLossMax]. The radical species taken into account for the calculation of the G-value are those produced along the path of the primary particle up to an energy loss between [eLossMin, eLossMax]. The initial value, eLossMin, sets a lower threshold for the energy loss of the primary particle. The primary particle is stopped when it has lost more energy than eLossMin. If the total energy deposition of an event (including the primary particle and all ejected electrons) is more than eLossMax, which is the maximum energy loss allowed, then the event is ignored in the simulation.³¹ This upper limit is used to prevent large energy deposition events (mainly caused by rare high-energy secondary particles) and therefore minimize simulation time. Since the range of energy loss limits these simulations, the volume of water chosen is large enough to encompass all the species produced. The advantage of this method is that the simulation is independent of geometry, and the total energy deposition is determined by eLossMin. However, eLossMin should be chosen to be large enough so that it can accurately simulate the full track structure characteristics at a given linear energy transfer (LET).
- II. The second method is to define a restricted simulation volume in which energy loss and chemical species produced are constrained. While the volume of these simulations must be small enough to limit energy loss and the number of chemical species, it should also be large enough to encompass the track structures of secondaries, especially at high ion energies.

Figure 5 shows an example of the time evolution of G-values for the first method [eLossMin = 10 keV, eLossMax = 10.1 keV] using nine main reactions (Table 4) for three existing microscopic models (IRT, IRT-syn, SBS) using the “chem6” example. The evolution of chemical species in heterogeneous distributions (ideally up to 1 μs) can be sufficiently described by these nine fast reactions (high constant rate and high concentration)^{22,31,62,66} The inclusion of a considerable number of secondary reactions is required when extending the time to include homogeneous chemistry for secondary chemical species and interactions with the medium (such as oxygen).⁶⁷ In these results, the statistical uncertainty is kept below 1% in all simulations by ensuring that a sufficiently large number of individual incident particles is shot on the irradiated medium. The relative computational time calculated between simulations using IRT, IRT-syn, and SBS is shown in Figure 6.

The G-value differences observed between the SBS and IRT approaches at longer times (up to about 1 μs) have been discussed in detail by Ramos-Méndez et al.²³ Briefly, these differences might be attributed in part to the independent pair approximation which is assumed by the IRT model. On the contrary, the SBS model considers a multiparticle system. Additionally, with a 95% (default) confidence level for a “free” jump (chemical species are free to diffuse during the time step), the SBS dynamic time step model assumes a 5% probability of missing encounters (or reactions) during the jump. Moreover, the default Minimum Time Step used in the simulation results of Figure 5 is 1 picosecond (this value can be changed by the user). During this time step, the Brownian Bridge technique is used to calculate the probability of the reaction, but the reaction of its products with surrounding reactants is not taken into account. This time step resolution can thus also lead to missing reactions. Unfortunately, increasing the confidence level of the “free” jump or decreasing the minimum time step can result in significantly longer computation times.

Benchmarking activities against existing simulation codes and experimental data began as early as the first released version with the SBS model,^{21,22,31} the IRT²³ and the IRT-syn⁴⁸ models. These activities may be boosted by user interfaces of TOPAS/TOPAS-nBio,^{62,71} that wrap and extend Geant4.

5.2 | Radio-sensitizing nanoparticles

One possible application of Geant4-DNA chemistry is to study the increase in radiochemical yields following an increase in energy deposition caused by radiosensitizing nanoparticles.⁷² The distributions of radio-induced chemical species (H_3O^+ , OH^- , $\cdot\text{OH}$, e^-_{aq} , H^+ , H_2 , H_2O_2) produced by scattered radiation from gold nanoparticles

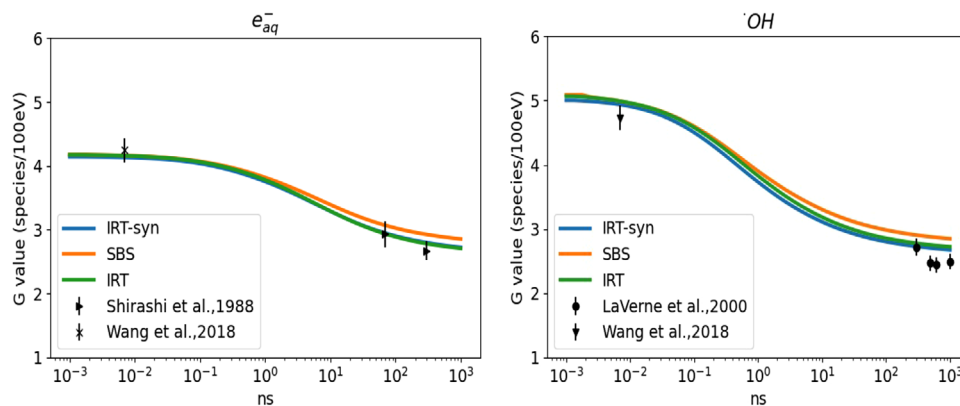


FIGURE 5 G-values of e^-_{aq} and $^{\cdot}OH$ as a function of time for the IRT, IRT-syn, and SBS models, considering the 9 chemical reactions of Table 4, for 1 MeV incident electrons with [eLossMin = 10 keV, eLossMax = 10.1 keV], compared to experimental data.^{68–70}

TABLE 4 The reactions and reaction rate coefficients used by IRT and IRT-syn are assigned for partially diffusion-controlled and totally diffusion-controlled reactions

Reaction	k ($\times 10^{10} \text{ M}^{-1} \text{ s}^{-1}$)	Partially diffusion-controlled	Totally diffusion-controlled
$H^{\cdot} + e^-_{aq} + H_2O \rightarrow OH^- + H_2$	2.5		X
$H^{\cdot} + ^{\cdot}OH \rightarrow H_2O$	1.55	X	
$H^{\cdot} + H^{\cdot} \rightarrow H_2$	0.503		X
$H_2O_2 + e^-_{aq} \rightarrow OH^- + ^{\cdot}OH$	1.1	X	
$H_3O^+ + e^-_{aq} \rightarrow H^{\cdot} + H_2O$	2.11	X	
$H_3O^+ + OH^- \rightarrow 2H_2O$	11.3		X
$^{\cdot}OH + e^-_{aq} \rightarrow OH^-$	2.95	X	
$^{\cdot}OH + ^{\cdot}OH \rightarrow H_2O_2$	0.55	X	
$e^-_{aq} + e^-_{aq} + 2H_2O \rightarrow 2OH^- + H_2$	0.636		X

Note: SBS considers that all reactions are totally diffusion-controlled reactions (see section 4.1.2).

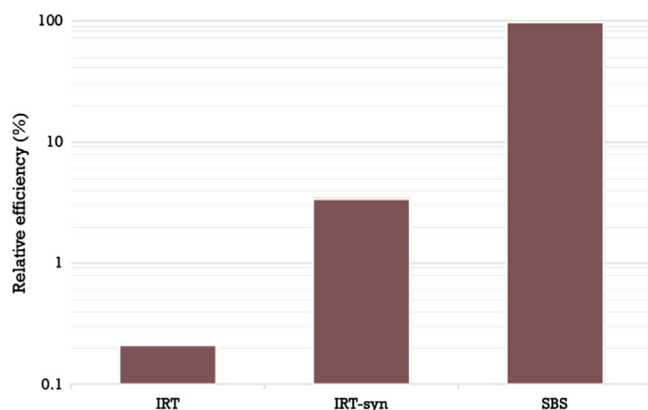


FIGURE 6 Relative computation times for IRT, IRT-syn, and SBS.

and their temporal evolution from 1 ps to 1 μ s, as a function of radial distance from the gold nanoparticle (GNP), can contribute to understanding the possible benefits of using GNPs. In this application, the compatibility of the chemistry module with the Geant4 design was demonstrated by a combination of Geant4 physics standard

models (*G4BraggModel* and the *G4BetheBlochModel*) and Geant4-DNA physics (track-structure), physico-chemical and chemical modeling capabilities for a single simulation. Recently, new gold discrete models have been implemented in Geant4-DNA^{73–75} and have been included in the “AuNP” example dedicated to track structure simulations in GNP.

5.3 | High dose rate irradiation

In recent years, studies on FLASH radiotherapy have highlighted the need to apply Monte Carlo simulations at high-dose rates. Such simulations could enable us to study how the inter-track effects in the chemical phase may be linked to the biological response observed (better healthy tissue preservation while maintaining tumor control). Since the computation time required for microscopic models (SBS, IRT) remains the main drawback of simulations involving a large number of species or long-time scales under high-dose-rate irradiation, the combination of microscopic models (SBS) and spatially heterogeneous concentration fields

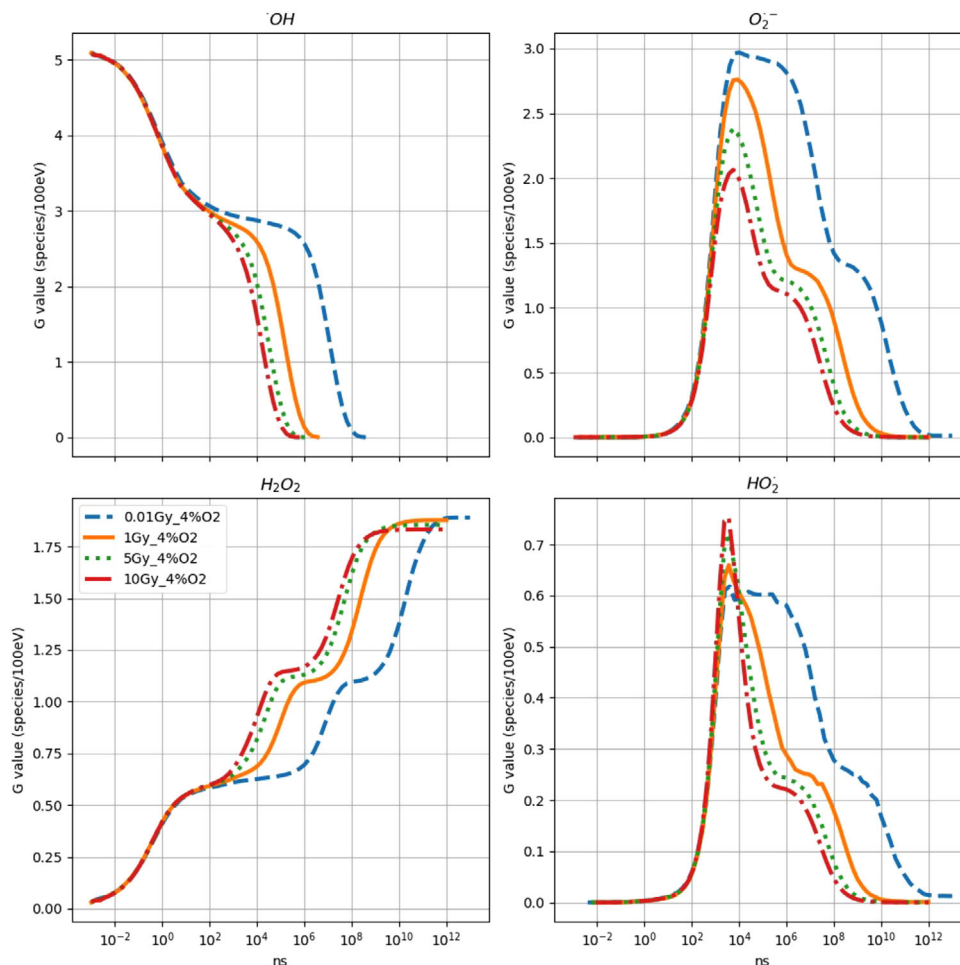


FIGURE 7 Comparison of G-values computed for different doses under instantaneous pulse conditions with 4% oxygenated water.

of the RDME model²⁷ at the mesoscopic scale has been implemented in Geant4-DNA to describe the evolution of water radiolysis simulation beyond the microsecond (see Section 4.2). Although the extension to homogeneous chemistry introduces the complexity of secondary reaction equations and acid-base-dependent kinetic equations, it could provide a better understanding of reactive oxygen species (ROS) ($\text{HO}_2^\bullet/\text{O}_2^{\bullet-}$) mechanisms by radiolysis in oxygenated water. A more detailed review is available in.⁷⁶

A new example called “UHDR” has been released in Geant4 11.2 for radiolysis simulation at high absorbed dose²⁷ by instantaneous pulse irradiation. By default, this example defines a 1 MeV electron source randomly placed on one of the faces of cubic oxygenated water volumes to accumulate absorbed doses. Instantaneous pulse irradiation means that electrons are shot together simultaneously. Two geometrical setups are proposed: one is a cubic water volume of $3.2 \times 3.2 \times 3.2 \mu\text{m}^3$ for a dose up to 0.01 Gy, the other one is a smaller cubic water volume of $1.6 \times 1.6 \times 1.6 \mu\text{m}^3$ for higher doses of up to 1, 5, or 10 Gy. As energy deposition is proportional to volume size for an absorbed dose,

and at microscale, the absorbed dose depends on the target size, the choice of simulation volume is a compromise between a sufficient number of chemical species and an achievable computational time. Users can use a dedicated interface available in the “UHDR” example to calculate the absorbed dose. Once a desired dose has been reached, all the primary chemical species induced by electron irradiation are produced simultaneously at 1 ps. Note that in these simulations, we considered that molecules diffuse and react within a volume limited by geometrical boundaries. These conditions enabled us to confine the chemical molecules in the considered volume by making them bounce off the walls of the volume. Figure 7 shows the results of time-dependent G-values for $^\circ\text{OH}$, HO_2^\bullet , $\text{O}_2^{\bullet-}$, and H_2O_2 in a 4% oxygenated water. The simulation covers a duration of up to 15 min after irradiation under $\text{pH} = 5.5$. The statistical uncertainty is kept below 1% in all simulations by ensuring that a sufficiently large number of individual bunches of electrons (called “events”) are shot onto the medium, each event delivering the chosen absorbed dose to the medium. The average computation time using a CPU Intel® Xeon® Gold 5220R CPU @ 2.20 GHz ranges

from 2.5 min to 5.5 h per event for the lower and higher doses, respectively.

5.4 | Early DNA damage

Geant4-DNA is an extension of Geant4 to study the mechanism of radiobiological effects at (sub-)cellular scale. Therefore, in recent years, efforts have been made to implement geometries of biological targets, such as DNA molecules, to understand and predict the consequences of irradiation at such a scale.^{48,49,77–79} These geometries of biological targets precisely describe the volumes of their constituents and their relative position can be used as a reaction center to define not only the direct effect of physical interactions but also the indirect effect of chemical reactions. The reaction model of radical species with DNA is primarily based on the assumption that DNA reaction centers are independent of the DNA molecule and that the macroscopic structure of DNA molecules does not affect the Brownian diffusion of radical species. The duration of the chemical stage is usually short enough (1–5 ns) or modeled as scavenging to involve only the generation of early DNA damage, which is still characterized by microscopic spurs along the track structure and limits the effects of a complex biological environment on the products of water radiolysis.

Geant4-DNA provides the example applications “dnadamage1”⁷⁷ (from version 10.7), “dnadamage2”⁷⁸ (from version 11.2), “molecularDNA”⁴⁹ (from version 11.1) and “dsbandrepair” (from version 11.2), which allow quantitative predictions of early DNA damage (within a few nanoseconds) in terms of single-strand breaks (SSBs), double-strand breaks (DSBs) and the classification of more complex cluster lesions for different DNA structures, ranging from the nucleotide level to the entire human cell nucleus. Despite the limitations of the reaction model and of our knowledge of indirect effects, these applications can be used to compare Geant4-DNA predictions with literature data.

6 | CONCLUSION

The Geant4-DNA chemistry module offers the first free and open-source toolkit for simulating water radiolysis induced by radiation. The design of the initial code, the diffusion-reaction models, and the incorporation of new functionalities in this module respond not only to emerging scientific questions, but also to the stability, extensibility, and improvement requirements of a large scientific community over the last 10 years.

The capability of Geant4-DNA to simulate water radiolysis may play a crucial role in various fields, including radiation therapy, radiation protection, and understanding the effects of radiation on biological systems,

particularly when water is the primary component of living tissues. This is underlined by 12 out of the total 31 Geant4-DNA examples using the chemistry module (until version Geant4.11.2), and the existing MC systems developed on top of Geant4-DNA. Achieving this also necessitates substantial efforts from the Geant4-DNA collaboration to maintain the code, develop new features, and establish validation programs for chemical models against experimental data, along with creating a more user-friendly interface that will be proposed in the future.

ACKNOWLEDGMENTS

The authors gratefully acknowledge Dr. Mathieu Karamitros and Dr. Alfonso Mantero for their early developments of Geant4-DNA chemistry. The authors would like to thank Dr. Nathanael Lampe for valuable discussions. The authors thank Dr. Jay LaVerne for the G-value experimental data. This work was supported by ESA/BioRad3 funding through contract number 4000132935/21/NL/CRS (2021–2023). ND, WGS, and JRM were partially funded by NIH/NCI R01CA187003 and R01CA266419.

CONFLICT OF INTEREST STATEMENT

The authors declare no conflicts of interest.

ORCID

Hoang Ngoc Tran 

<https://orcid.org/0000-0002-9243-6842>


Jay Archer  <https://orcid.org/0009-0008-5248-5739>

Giuseppe Antonio Pablo Cirrone 

<https://orcid.org/0000-0001-5733-9281>

Naoki Dominguez 

<https://orcid.org/0000-0002-4410-1925>

Serena Fattori 

<https://orcid.org/0000-0002-9381-7620>

Wook-Geun Shin 

<https://orcid.org/0000-0002-8622-1888>

Sebastien Incerti 

<https://orcid.org/0000-0002-0619-2053>

REFERENCES

1. Friedland W, Jacob P, Bernhardt P, et al. Simulation of DNA damage after proton irradiation. *Radiat Res.* 2003;159:401–410.
2. Plante I, Cucinotta FA. Cross sections for the interactions of 1 eV–100 MeV electrons in liquid water and application to Monte-Carlo simulation of HZE radiation tracks. *New J Phys.* 2009;11:063047.
3. Krämer M, Kraft G. Calculations of heavy ion track structure. *Radiat Environ Biophys.* 1994;33:91–109.
4. Uehara S, Nikjoo H. Monte Carlo simulation of water radiolysis for low-energy charged particles. *J Radiat Res.* 2006;47:69–81.
5. Nikjoo H, Emfietzoglou D, Liamsuwan T, et al. Radiation track, DNA damage and response—a review. *Rep Prog Phys.* 2016;79:116601.
6. Cobut V, Frongillo Y, Patau JP, et al. Monte Carlo simulation of fast electron and proton tracks in liquid water-I. Physical and physicochemical aspects. *Radiat Phys Chem.* 1998;51:229–243.

7. Pimblott S, LaVerne JA, Mozumder A, et al. Structure of electron tracks in water. 1. Distribution of energy deposition events. *J Phys Chem*. 1990;94:488-495.
8. Schuemann J, McNamara AL, Ramos-Méndez J, et al. TOPAS-nBio: an extension to the TOPAS simulation toolkit for cellular and sub-cellular radiobiology. *Radiat Res*. 2018;191:125-138.
9. Incerti S, Kyriakou I, Bernal MA, et al. Geant4-DNA example applications for track structure simulations in liquid water: a report from the Geant4-DNA Project. *Med Phys*. 2018;45:e722-e739.
10. Incerti S, Ivanchenko A, Karamitros M, et al. Comparison of Geant4 very low energy cross section models with experimental data in water. *Med Phys*. 2010;37:4692-4708.
11. Bernal MA, Bordage MC, Brown JMC, et al. Track structure modeling in liquid water: a review of the Geant4-DNA very low energy extension of the Geant4 Monte Carlo simulation toolkit. *Phys Med: Eur J Med Phys*. 2015;31(8):861-874.
12. Incerti S, Baldacchino G, Bernal M, et al. The Geant4-DNA project. *Int J Model Simul Sci Comput*. 2010;1:157-178.
13. Kyriakou I, Sakata D, Tran HN, et al. Review of the Geant4-DNA simulation toolkit for radiobiological applications at the cellular and DNA level. *Cancers*. 2022;14:35.
14. Plante I. A review of simulation codes and approaches for radiation chemistry. *Phys Med Biol*. 2021;66:03TR02.
15. Agostinelli S, Allison J, Amako K, et al. GEANT4—a simulation toolkit. *Nucl Instrum Meth Phys Res A*. 2003;506(3):250-303.
16. Allison J, Amako K, Apostolakis J, et al. Geant4 developments and applications. *Nucl Sci IEEE Trans*. 2006;53:270-278.
17. Allison J, Amako K, Apostolakis J, et al. Recent developments in GEANT4. *Nucl Instrum Methods Phys Res A*. 2016;835:186-225.
18. Zein SA, Bordage M-C, Tran HN, et al. Monte Carlo simulations of electron interactions with the DNA molecule: a complete set of physics models for Geant4-DNA simulation toolkit. *Nucl Instrum Meth B*. 2023;542:51-60.
19. Zein SA, Bordage M-C, Francis Z. Electron transport in DNA bases: an extension of the Geant4-DNA Monte Carlo toolkit. *Nucl Instrum Meth B*. 2021;488:70-82.
20. Bug MU, Baek WY, Rabus H, et al. An electron-impact cross section data set (10eV–1 keV) of DNA constituents based on consistent experimental data: a requisite for Monte Carlo simulations. *Radiat Phys Chem*. 2017;130:459-479.
21. Karamitros M, Mantero A, Incerti S, et al. Modeling radiation chemistry in The Geant4 Toolkit. *Prog Nucl Sci Tech*. 2011;2:503-508.
22. Karamitros M, Luan S, Bernal MA, et al. Diffusion-controlled reactions modeling in Geant4-DNA. *J Comput Phys*. 2014;274:841-882.
23. Ramos-Méndez J, Shin WG, Karamitros M, et al. Independent reaction times method in Geant4-DNA: implementation and performance. *Med Phys*. 2020;47(11):5919-5930.
24. Chappuis F, Griji V, Tran HN, et al. Modeling of scavenging systems for water radiolysis with Geant4-DNA. *Phys Med*. 2023;108:102549.
25. D-Kondo JN, Garcia-Garcia OR, LaVerne JA. An integrated Monte Carlo track-structure simulation framework for modeling inter and intra-track effects on homogenous chemistry. *Phys Med Biol*. 2023;68:125008.
26. Camazzola G, Boscolo D, Scifoni E, et al. TRAX-CHEMxt: towards the homogeneous chemical stage of radiation damage. *Int J Mol Sci*. 2023;24:9398.
27. Tran HN, Chappuis F, Incerti S, et al. Geant4-DNA modeling of water radiolysis beyond the microsecond: an on-lattice stochastic approach. *Int J Mol Sci*. 2021;22:6023.
28. Michaud M, Wen A, Sanche L. Cross sections for low-energy (1–100 eV) electron elastic and inelastic scattering in amorphous ice. *Radiat Res*. 2003;159:3-22.
29. Melton C. Cross sections and interpretation of dissociative attachment reactions producing OH⁻, O⁻, and H⁻ in H₂O. *J Chem Phys*. 1972;57:4218.
30. Shin WG, Bordage M-C, Emfietzoglou D, et al. Development of a new Geant4-DNA electron elastic scattering model for liquid-phase water using the ELSEPA code. *J Appl Phys*. 2018;124:224901.
31. Shin W-G, Ramos-Méndez J, Faddegon BA, et al. Evaluation of the influence of physical and chemical parameters on water radiolysis simulations under MeV electron irradiation using Geant4-DNA. *J Appl Phys*. 2019;125:104301.
32. Meesungnoen J, Jay-Gerin J-P, Filali-Mouhim A, et al. Low-energy electron penetration range in liquid water. *Radiat Res*. 2002;158:657.
33. Michaud M, Sanche L. Absolute vibrational excitation cross sections for slow-electron (1–18 eV) scattering in solid H₂O. *Phys Rev A*. 1987;36:4684.
34. Michaud M, Sanche L. Total cross sections for slow-electron (1–20 eV) scattering in solid H₂O. *Phys Rev A*. 1987;36:4672.
35. Terrissol M, Beaudre A. Simulation of space and time evolution of radiolytic species induced by electrons in water. *Radiat Prot Dosim*. 1990;31:175-177.
36. Ritchie RH, Hamm RN, Turner dJE. Interactions of low-energy electrons with condensed matter: relevance for track structure. *Computational Approaches in Molecular Radiation Biology*. Springer; 1994.
37. Kreipl MS, Friedland W, Paretzke HG. Time- and space-resolved Monte Carlo study of water radiolysis for photon, electron and ion irradiation. *Radiat Environ Biophys*. 2009;48:11-20.
38. Shin W-G, Ramos-Mendez J, Tran NH, et al. Geant4-DNA simulation of the pre-chemical stage of water radiolysis and its impact on initial radiochemical yields. *Phys Med*. 2021;88:86-90.
39. Lu H, Long FH, Bowman RM, et al. Femtosecond studies of electron-cation geminate recombination in water. *J Phys Chem*. 1989;93:27-28.
40. Marshall W. Dielectric constant of water discovered to be simple function of density over extreme ranges from – 35 to + 600 °C and to 1200 MPa (12000 Atm.). *Believed Universal Nat Prec*. 2008. <https://www.nature.com/articles/npre.2008.2472.1#citeas>
41. Kreipl MS, Friedland W, Paretzke HG. Time- and space-resolved Monte Carlo study of water radiolysis for photon, electron and ion irradiation. *Radiat Environ Bio*. 2009;48(1):11-20.
42. Han P, Bartels DM. Hydrogen/deuterium isotope effects in water radiolysis. 2. Dissociation of electronically excited water. *J Phys Chem*. 1990;94:5824.
43. Karamitros M, Brown J, Lampe N, et al. Implementing the Independent Reaction Time Method in Geant4 for Radiation Chemistry Simulations. arXiv:2006.14225, 2020.
44. Clifford P, Green NJB, Oldfield MJ, et al. Stochastic models of multi-species kinetics in radiation-induced spurs. *J Chem SOC, Faraday Trans I*. 1986;82:2673-2689.
45. Michalik V, Begusová M, Bigildeev EA. Computer-aided stochastic modeling of the radiolysis of liquid water. *Radiat Res*. 1998;149(3):224-236.
46. Plante I, Devroye L. Considerations for the independent reaction times and step-by-step methods for radiation chemistry simulations. *Radiat Phys Chem*. 2017;139:157-172.
47. Green NJB, Pilling MJ, Pimblott SM, et al. Stochastic modeling of fast kinetics in a radiation track. *J Phys Chem*. 1990;94:251-258.
48. Tran HN, Ramos-Méndez J, Shin WG, et al. Assessment of DNA damage with a new Independent Reaction Time approach implemented in Geant4-DNA for the simulation of diffusion-controlled reactions between radio-induced reactive species and a chromatin fiber. *Med Phys*. 2021;48:890-901.
49. Lampe N, Karamitros M, Breton V, et al. Mechanistic DNA damage simulations in Geant4-DNA part 1: a parameter study in a simplified geometry. *Phys Med*. 2018;48:P135-145.
50. Elf J, Ehrenberg M. Spontaneous separation of bi-stable biochemical systems into spatial domains of opposite phases. *Syst Biol (Stevenage)*. 2004;1(2):230-236.

51. Gillespie D. Exact stochastic simulation of coupled chemical reactions. *J Phys Chem*. 1977;81(25):2340-2361.
52. Gillespie D, Hellander A, Petzold L. Perspective: stochastic algorithms for chemical kinetics. *J Chem Phys*. 2013;138:170901.
53. Hellander S, Hellander A. Hierarchical algorithm for the reaction-diffusion master equation. *J Chem Phys*. 2020;152:034104.
54. Pimblott SM, Pilling MJ, Green NJ. Stochastic models of spur kinetics in water. *Int J Radiat Appl Instrum Part Radiat Phys Chem*. 1991;37:377-388.
55. Bian J, Duran J, Shin WG, et al. GEANT4-DNA simulation of temperature-dependent and pH-dependent yields of chemical radiolytic species. *Phys Med Biol*. 2023;68:124002.
56. Ferradini C, Jay-Gerin JP. The effect of pH on water radiolysis: a still open question—a minireview. *Res Chem Inter*. 2000;26:549.
57. Roth O, LaVerne JA. Effect of pH on H₂O₂ production in the radiolysis of water. *J Phys Chem A*. 2011;115(5):700-708.
58. Pastina B, LaVerne JA. Effect of molecular hydrogen on hydrogen peroxide in water radiolysis. *J Phys Chem A*. 2001;105:9316-9322.
59. Sultana A, Alanazi A, Meesungnoen J, et al. Generation of ultrafast, transient, highly acidic pH spikes in the radiolysis of water at very high dose rates: relevance for FLASH radiotherapy. *Can J Chem*. 2022;100:272-279.
60. Elliot AJ, Bartels DM. *The reaction set, rate constants and g-values for the simulation of the radiolysis of light water over the range 20 deg to 350 deg C based on information available in 2008*. AECL153-127160-450-001; Atomic Energy of Canada Limited: Mississauga, ON, Canada.
61. Hervé du Penhoat M-A, Goulet T, Frongillo Y, et al. Radiolysis of liquid water at temperatures up to 300 C: a Monte Carlo simulation study. *J Phys Chem A*. 2000;104:11757-11770.
62. Ramos-Méndez J, Perl J, Schuemann J, et al. Monte Carlo simulation of chemistry following radiolysis with TOPAS-nBio. *Phys Med Biol*. 2018;63:105014.
63. Brun R, Rademakers F. ROOT—an object-oriented data analysis framework. *Nucl Inst Meth in Phys Res A*. 1997;389:81-86.
64. Thomas DJ. ICRU report 85: fundamental quantities and units for ionizing radiation. *Radiat Prot Dosim*. 2012;150(4):550-552.
65. LaVerne JA, Štefanić I, Pimblott SM. Hydrated electron yields in the heavy ion radiolysis of water. *J Phys Chem A*. 2005;109:9393-9401.
66. Pimblott SM. Investigation of various factors influencing the effect of scavengers on the radiation chemistry following the high-energy electron radiolysis of water. *J Phys Chem*. 1992;96:4485-4491.
67. Elliot AJ, McCracken DR. Computer modelling of the radiolysis in an aqueous lithium salt blanket: suppression of radiolysis by addition of hydrogen. *Fusion Eng Des*. 1990;13:21-27.
68. Wang F, Schmidhammer U, Larbre JP, et al. Time-dependent yield of the hydrated electron and the hydroxyl radical in D₂O: a picosecond pulse radiolysis study. *Phys Chem Chem Phys*. 2018;20:15671-15679.
69. Laverne JA. OH radicals and oxidizing products in the gamma radiolysis of water. *Radiat Res*. 2000;153:196-200. <http://jstor.org/stable/3580071>
70. Shiraishi H, Katsumura Y, Hiroishi D, et al. Pulse-radiolysis study on the yield of hydrated electron at elevated temperatures. *J Phys Chem*. 1988;92:3011-3017.
71. Ramos-Mendez JA, LaVerne JA, Domínguez-Kondo JN, et al. 2021 TOPAS-nBio validation for simulating water radiolysis and DNA damage under low-LET irradiation. *Phys Med Biol*. 2021;66:175026.
72. Tran HN, Karamitros M, Ivantchenko V, et al. Geant4 Monte Carlo simulation of absorbed dose and radiolysis yields enhancement from a gold nanoparticle under MeV proton irradiation. *Nucl Instrum Meth B*. 2016;373:126-139.
73. Sakata D, Incerti S, Bordage MC, et al. An implementation of discrete electron transport models for gold in the Geant4 simulation toolkit. *J Appl Phys*. 2016;120:244901.
74. Sakata D, Kyriakou I, Okada S, et al. Geant4-DNA track-structure simulations for gold nanoparticles: the importance of electron discrete models in nanometer volumes. *Med Phys*. 2018;45:2230-2242.
75. Sakata D, Kyriakou I, Tran HN, et al. Electron track structure simulations in a gold nanoparticle using Geant4-DNA. *Phys Med*. 2019;63:98-104.
76. Chappuis F, Tran HN, Zein SA, et al. The general-purpose geant4 monte carlo toolkit and its geant4-dna extension to investigate mechanisms underlying the FLASH effect in radiotherapy: Current status and challenges. *Phys Med*. 2023;110:102601.
77. Meylan S, Incerti S, Karamitros M, et al. Simulation of early DNA damage after the irradiation of a Fibroblast cell nucleus using Geant4-DNA. *Sci Rep*. 2017;7:11923.
78. D-Kondo N, Moreno-Barbosa E, Štěpán V, et al. DNA damage modeled with Geant4-DNA: effects of plasmid DNA conformation and experimental conditions. *Phys Med Biol*. 2021;66:245017.
79. Ballisat L, Beck L, De Sio C, et al. In-silico calculations of DNA damage induced by alpha-particles in the 224Ra DaRT decay chain for a better understanding of the radiobiological effectiveness of this treatment. *Phys Med*. 2023;112:102626.

How to cite this article: Tran HN, Archer J, Baldacchino G, et al. Review of chemical models and applications in Geant4-DNA: Report from the ESA BioRad III Project. *Med Phys*. 2024;1-17. <https://doi.org/10.1002/mp.17256>